ChemPubSoc Europe

DOI: 10.1002/chem.201501348

CHEMISTRY A European Journal Full Paper

Photoinduced CO Release

Photoinduced Carbon Monoxide Release from Half-Sandwich Iron(II) Carbonyl Complexes by Visible Irradiation: Kinetic Analysis and Mechanistic Investigation

Xiujuan Jiang,[a] Limei Chen,[b] Xiu Wang,[a] Li Long,[a] Zhiyin Xiao,[a] and Xiaoming Liu*[a, b]

Abstract: Three half-sandwich iron(II) complexes, [Fe(η^5-Cp)(*cis*-CO)$_2$X] ($X^- = Cl^-$, Br^-, I^-), were synthesized and characterized. The kinetics of the CO-releasing behaviour of these complexes upon illumination by visible irradiation in various media was investigated. Our results indicated that the CO release was significantly affected by the auxiliary ligands. Of the three light sources used (blue, green, and red), blue light exhibited the highest efficiency. In the photoinduced CO release, the solvents and exogenous nucleophiles in the media were involved, which allowed their CO-releasing reaction to comply with pseudo first-order model rather than the characteristic zero-order model for a photochemical reaction. In aqueous media (D_2O), an intermediate bearing the core of {Fe^{II}(*cis*-CO)$_2$} involving cleavage of cyclopentadiene was detected. Despite the non-absorption of the red light, its illumination combined with nucleophilic substitution did cause considerable CO release. Assessment of the cytotoxicity of the three complexes indicated that they showed good biocompatibility.

Introduction

Carbon monoxide (CO) has been recognized as a biological effector in human bodies, possessing multiple biological functions, such as anti-inflammatory, anti-apoptotic, anti-bacteria.[1] Inhalation of CO gas under controlled conditions alleviates symptoms of human pulmonary hypertension[2] and appears also to protect vital organs such as the brain, heart, lung, and liver during ischemia/hypoxia and organ transplantation.[3] In fact, there has been a long history of employing CO clinically.[4] Owing to the poisoning hazard, direct inhalation of CO has not been clinically favoured. To fully exploit the medical application of CO, safe and controllable CO delivery is highly desired. Such a CO delivery requires a CO carrier from which CO can be controllably released on-site and on-request. The CO carrier was dubbed a CORM (CO-releasing molecule).[5] Among the inorganic and organic candidates as CORMs, metal carbonyl complexes have attracted particular attention over the past decade.[6] Compared to an organic CORM,[7] not only do metal carbonyl complexes have increased CO-loading capacity, possessing possibly as many as six CO molecules per metal complex, but also offer vast options as potential CORMs.

As an ideal CORM, one of the criteria is that there should be an appropriate approach to the controllably release of its CO besides the requirements of minimum cytotoxicity from both itself and any residues post-CO-release. As far as the chemical nature of CO release is concerned, any method leading to the metal–CO bond breakage can be employed to initiate CO release. In the past decade, a number of approaches have been reported, including hydrolysis or ligand substitution,[5,8] enzymatic degradation,[9] redox induction,[10] and photoactivation.[11] Among the reported approaches for CO release, photoinduction has a number of advantages over the others. It does not introduce additional compounds into the CO-releasing system except for the CORM itself and residues from its decomposition. The CO release is highly controllable, which is achieved by simply switching on/off photoirradiation and controlling the illuminating time. Such a CORM is dubbed PhotoCORM. However, from the viewpoint of clinic application, there is a major challenge for PhotoCORMs, namely, the selection of irradiation. Depending on the structural and electronic natures of the PhotoCORMs, particularly the strength of the M–CO bond, the irradiation required to initiate the photochemistry must in general be either in the ultraviolet region or the short wavelength region end of visible light. However, such wavelengths barely penetrate body tissues and are thus of practically no use in clinic applications. Body tissues are relatively transparent to irradiation in the near-IR region, but such irradiation is unable to directly induce CO release from PhotoCORMs owing to its low energy. On the other hand, the irradiation of long wavelengths, for example, longer than 600 nm in the visible region, are absorbed much less by body tissues compared

[a] Dr. X. Jiang, X. Wang, L. Long, Z. Xiao, Prof. Dr. X. Liu
College of Biological, Chemical Sciences and Engineering
Jiaxing University, Jiaxing (P. R. China)
Fax: (+86) 573-8364-3937
E-mail: xiaoming.liu@mail.zjxu.edu.cn

[b] L. Chen, Prof. Dr. X. Liu
School of Metallurgy and Chemical Engineering
Jiangxi University of Science and Technology
Ganzhou (P. R. China)

Supporting information for this article is available on the WWW under http://dx.doi.org/10.1002/chem.201501348.

to those of short wavelengths. Therefore, exploiting metal complexes which absorb irradiation of long wavelengths in the visible region may be of importance in exploring novel Photo-CORMs.

Iron is arguably more biocompatible compared to other transition metals as it is one of the essential elements in the life cycle of many life forms, including humans. Having many years research experience working on diiron carbonyl complexes as the mimics of the diiron subunit of [FeFe]-hydrogenase and their high CO content per molecule,[12] we have been interested in exploiting their potentials as CORMs. It has been found that those diiron carbonyl complexes could release CO by using a substitution–induction procedure, but they are inert to photoinduction. Iron(II) carbonyl complexes bearing the core {Fe(*cis*-CO)$_2$} are a large well-documented category of complexes.[13] One distinct feature of these complexes is their light sensitivity. One famous example is the mono-iron(II) centre of [Fe]-hydrogenase, which degrades upon UV irradiation.[14] Their photosensitivity seems to be associated with their ancillary ligand(s). The σ-donating, π-accepting/donating capability of the ancillary ligands would exert profound influence on the photosensitivity and absorption on visible light by the electron density on the iron centre and thus the bond strength of the Fe^{II}–CO moiety.

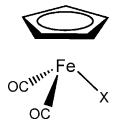

Figure 1. The three half-sandwich iron(II) carbonyl complexes **1**–**3**, where X$^-$ = Cl$^-$ (**1**), Br$^-$ (**2**), I$^-$ (**3**).

Herein, we report the photoinduced CO-releasing behaviour of three half-sandwich iron(II) complexes, namely [Fe(η^5-Cp)(*cis*-CO)$_2$X] with X$^-$ = Cl$^-$ (**1**), Br$^-$ (**2**), I$^-$ (**3**)[15] (Figure 1) in various media, DMSO, deuterated water (D_2O), and physiological saline/D_2O. Their photoinduced CO release was investigated using three LED lights (blue, λ = 470–475 nm; green, λ = 492–577 nm; and red, λ = 622–770 nm). It turned out that the blue light was the most efficient whereas the red light showed the poorest efficiency for photoinduced CO release. Their CO-releasing behaviour correlated also to the second ancillary ligand X (X$^-$ = Cl$^-$, Br$^-$, I$^-$). Additionally, solvents and the Cl$^-$ in the saline were also involved in their decomposition to release CO in a concerted manner with the photoinduction, which rendered their CO release a pseudo first-order kinetic process. In a non-polar and non-coordinating solvent, their CO-release kinetics complied with a zero-order model, as expected for a photochemical reaction.

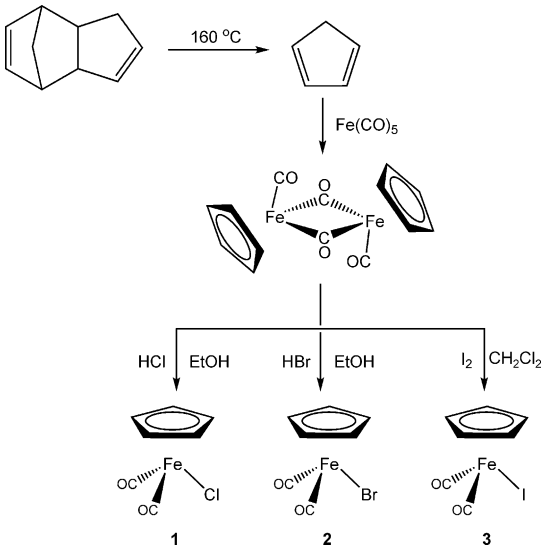

Scheme 1. The synthetic routes to complexes **1**–**3**.

Results and Discussion

Synthesis and characterisation of complexes 1–3

Complexes **1**–**3** were synthesised using the procedures reported previously with modifications when necessary (Scheme 1).[15] In the synthesis of complexes **1** and **2**, the strongly corrosive reagents, $SOCl_2$ and Br_2, were replaced by HCl and HBr, respectively. The replacement allowed for the synthesis to be conducted in one-pot manner rather than dropwise addition of the corrosive $SOCl_2$/Br_2. Complex **3** was synthesised by the reaction of [CpFe(μ-CO)(CO)]$_2$ with I_2 in CH_2Cl_2 by following the reported method.[15c]

All of these complexes are soluble in common organic solvents, such as DMSO, CH_2Cl_2, and CH_3CN. Additionally, these complexes are stable in the dark at room temperature. However, they are sensitive to daylight and subject to decomposition upon irradiation. The IR absorption bands of the complexes are shown in Figure 2. These complexes possess the characteristic IR absorption bands for Fe^{II} complexes with two CO bound *cis* to each other (complex **1**: 2043, 1993 cm^{-1}; complex **2**: 2039, 1990 cm^{-1}; complex **3**: 2032, 1984 cm^{-1}).[13] From complexes 1 to 3, the absorption bands shift steadily to low frequency by a few wavenumbers. The red-shift of the characteristic IR absorption peaks can be attributed to the increase in electron-donating capability from Cl$^-$ to I$^-$. The UV/Vis absorption spectra of complexes **1**–**3** show rich absorption bands

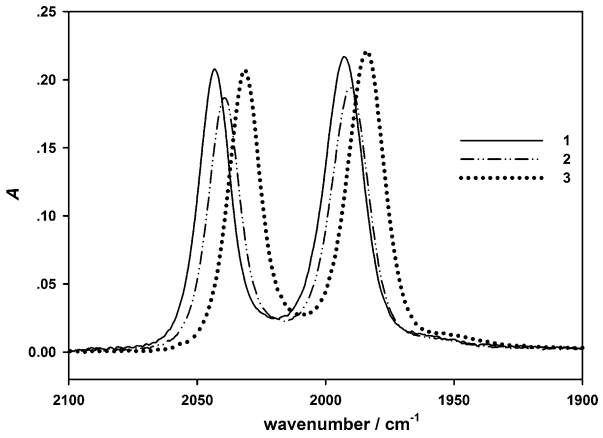

Figure 2. The ν(CO) region of the IR spectra for complexes **1**–**3** in DMSO.

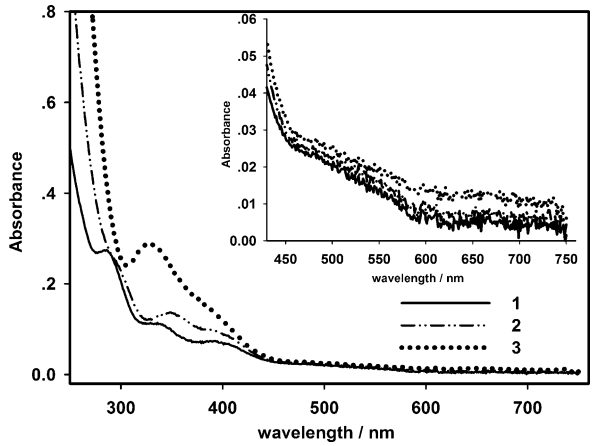

Figure 3. The UV/Vis absorption spectra of complexes **1**–**3** examined in CH_3CN (inset: spectra between 430–750 nm).

from 250 to 450 nm (Figure 3). These bands may be a mixture of ligand-based transition and metal-to-ligand charge transfer (MLCT). It is noteworthy that the tailing of the spectra extends beyond 450 nm and up to 600 nm. The tails of the absorption bands penetrate into the visible region, which renders the possibility of using visible light to excite these complexes.

Being excited by visible light is one thing, but whether the excitation leads to photoinduced CO release is another. In fact, diiron hexacarbonyl complexes show rather similar UV/Vis spectra to those of complexes **1**–**3**, but they have turned out to be rather photostable. To explain such a difference, those factors that affect the stability of the excited state of a complex need to be established. Amongst the factors, the energy level of the LUMO of a complex ought to play a crucial role. The higher the energy levels of the LUMO into which the electron is excited, the more vulnerable the complex to photoinduced decomposition. It is well-known that the energy level of a LUMO is correlated to the reduction potential of a complex.[16] Thus, we examine the electrochemistry of the three complexes. The cyclic voltammograms are shown in Figure 4. The process at about −1.3 V is assigned to $Fe^{II} \rightarrow Fe^{I}$. The second redox

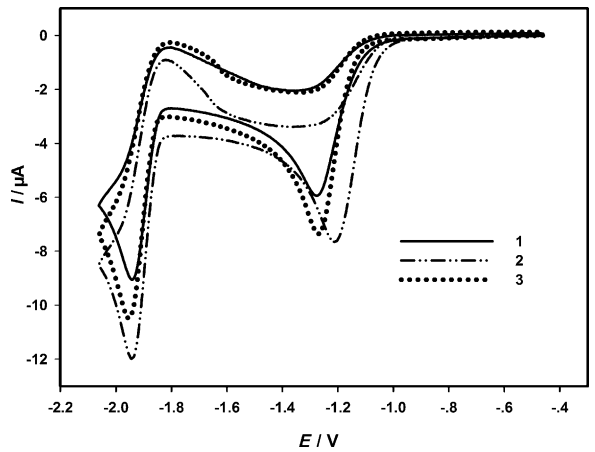

Figure 4. Cyclic voltammograms of complexes **1**–**3** in $[nBu_4N]BF_4$–CH_3CN under an Ar atmosphere (298 K, scanning rate = 0.1 V s^{-1}).

event originated from the product of the chemical reaction of the reduced species, $[(\eta^5\text{-Cp})Fe^{I}(cis\text{-CO})_2X]^-$. The reduced species may lose the halide to dimerise to form the precursor $[[(\eta^5\text{-Cp})Fe^{I}(\mu\text{-CO})(CO)]_2]$. This was further confirmed by the observation that adding the precursor to the system enhanced the second process (Supporting Information, Figure S1). Indeed, the reduction potentials of these complexes are more negative by about 200–300 mV compared to diiron hexacarbonyl complexes.[8b] The correlation suggests that diiron penta- or tetracarbonyl complexes may be of the potential use as PhotoCORM, although the hexacarbonyl analogues are photoinert.

Photoinduced CO release from complexes 1–3 in DMSO and kinetic analysis

To examine the photosensitivity of the three complexes, three light sources (blue, green, and red LED lights) were used. Steady progress of the reaction is indicated by the decrease in the intensity of IR absorption bands of the bound CO (Figure 5

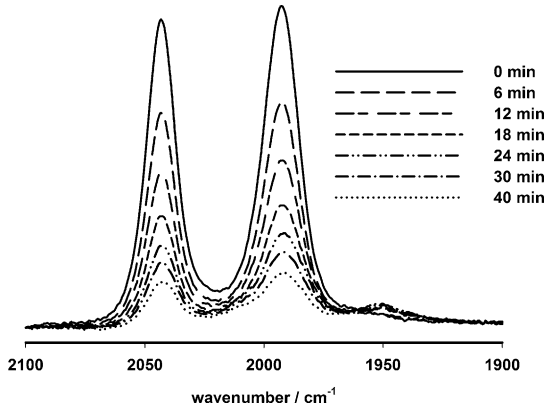

Figure 5. Variation of IR spectra during the decomposition of complex **1** (0.013 mol L^{-1}) upon blue-light irradiation in DMSO under open atmosphere.

and Supporting Information, Figures S2 and S3) under irradiation of the blue light. The other two lights also caused photoinduced decomposition, although the reactions were much slower (Supporting Information, Figures S4–S9).

It is possible to form the dimer precursor of complexes **1**–**3** if photoinduced Fe–X hemolytic cleavage occurs. To confirm this possibility, the photoactivity of the precursor was checked in DMSO using blue light (Supporting Information, Figure S10). It was found that its photoinduced decomposition was much slower than its derived complexes. Therefore, it is clear that reforming the precursor is not the major product, if indeed it is involved at all. To examine further what the decomposition product might be, the photoinduced CO-releasing reaction of complex **1** was also carried out in deuterated DMSO and examined using NMR spectroscopy (Figure 6). Given that the Fe^{II} in these complexes is bound to the Cp ring in an η^5 manner, the complexes showed only one signal. For complex **1**, the signal was at δ, 5.3 ppm. This signal gradually weakened and ultimate

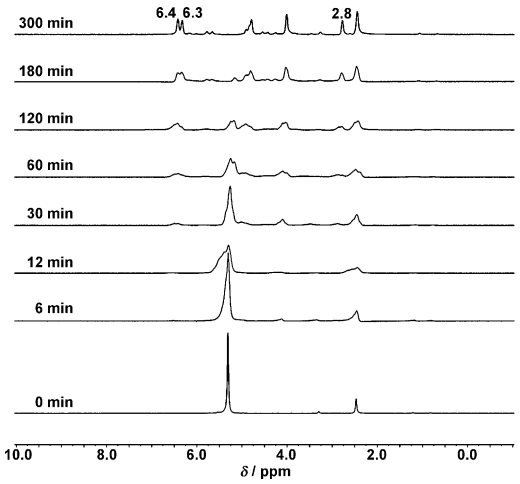

Figure 6. Variation ^{1}H NMR spectra with reaction time of complex **1** under blue-light illumination.

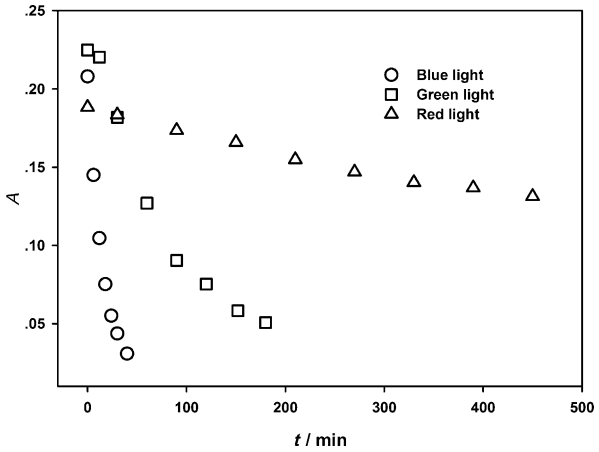

Figure 7. Plots of the absorption at 2043 cm^{-1} of complex **1** (0.013 mol L^{-1}) against the reaction time in DMSO under open atmosphere.

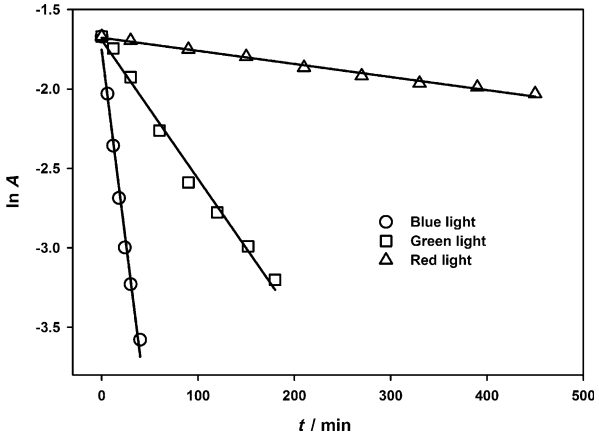

Figure 8. Logarithmic plots of the absorption at 2043 cm^{-1} of complex **1** (0.013 mol L^{-1}) against reaction time in DMSO under open atmosphere.

disappeared as the reaction proceeded, which indicated the complete decomposition of complex **1**. The photoinduced reaction was readily detectable as indicated by the NMR spectrum shown in Figure 6. The three signals at δ, 6.4, 6.3, and 2.8 ppm are assigned to free cyclopentadiene.[17] Furthermore, the ^{13}C NMR signals at δ, 134, 133, and 42 ppm in the spectrum (Supporting Information, Figure S11) of the decomposed products of complex **1**[18] and the GC-MS analysis (Supporting Information, Figure S12) also confirmed the presence of the free cyclopentadiene. The mass spectra of complex **1** under various conditions were very similar in their spectral patterns (Supporting Information, Figure S13). It is noteworthy that the signals matching the fragments dimerised cyclopentadiene (m/z=133, $C_{10}H_{12}+H^+$), chlorocyclopentadiene (m/z=100.5, $C_5H_5Cl+H^+$) are not observed or appear rather weak (Supporting Information, Figure S13, top) in the mass spectrum of the complex **1** in water without illumination. The other three main groups of signals at 178, 214, and 256 are all present with drastic difference in their relative intensities. The signals around 214 and 178 are readily assigned to the complex itself and the product with the chloride depleted, respectively. The signal around 256 are highly likely associated to the species which is the chloride-depleted fragment (mass 178) bound with a DMSO molecule, auxiliary solvent always used at minimum for helping dissolving the complex either in water or saline. In water without illumination, the latter two signals (214 and 256) are much stronger. Their intensities are apparently associated with the concentration of the complex, which explains why they are rather strong without illumination in water (Supporting Information, Figure S13, top). The presence of the dimerised cyclopentadiene is also in agreement with the instability of free cyclopentadiene. The unmarked signals might be associated with the Cp ring remaining bound to the metal centre. The results indicate that the metal centre remained in oxidation state II despite the complicated decomposing pathways.

Kinetic analysis was performed for the photoinduced decomposition of complexes **1**–**3**. Variations in the absorbance of complex **1** along the reaction course are shown in Figure 7. As shown in Figure 7, the spectral variation showed exponential trends which are not the characteristic of photochemical decomposition. Indeed, regression of the data to a first-order reaction model gave a linear plot for complex **1** under the irradiation of the three lights (Figure 8). Analogous plots for complexes **2** and **3** were also obtained (Supporting Information, Figures S14 and S15). All the kinetic data were summarized in Table 1. As shown in Table 1, of the three light sources, the blue light was the most efficient and the red light the least efficient in inducing the decomposition of these complexes. This echoes accordingly the spectral features of their UV/Vis spectral profiles (Figure 3).

The results indicated that the photoinduced CO release is significantly affected by the auxiliary ligand, namely the halides. In general, complex **1** with a chloride is the most readily subject to photoinduction to decompose whereas complex **3**, which possesses an iodide, is the most inert against photoinduction among the three complexes. This variation is probably due to the bonding nature of the bond Fe^{II}–X (X = Cl^-, Br^-, I^-). It is known that from Cl^- to I^-, there are at least three variation

Table 1. Kinetic data of the photoinduced decomposition of complexes **1**–**3** (0.013 mol L^{-1}) in DMSO upon illumination with various LEDs under open atmosphere in DMSO.

Complex	$k_{obs} \times 10^3$ ($t_{1/2}$ [min])			
	Blue	Green	Red	Daylight
1	42.0 ± 5.4 (17)	9.0 ± 0.3 (77)	0.83 ± 0.06 (835)	0.4 (1733)
2	34.4 ± 4.5 (20)	8.4 ± 0.4 (83)	1.33 ± 0.06 (521)	0.3 (2310)
3	30.2 ± 3.4 (23)	8.2 ± 0.6 (85)	4.8 ± 0.4 (144)	0.4 (1733)

trends, increases in ionic radius, tendency of donating electron (energy level of their frontier orbital), and their polarisability. The consequence is that from Cl^- to I^-, the covalent character of the Fe^{II}–X bonds increases. The observation implies that decreasing the covalent character of the Fe^{II}–X bond would be beneficial to enhancing photoinduced CO release when introducing an auxiliary ligand. In other words, introducing the third ligand could be an effective manner to tune the photoinduced CO release. However, this behaviour was at odds with what was observed when the red light was employed (Table 1). The above trend was completely reversed. In this situation, complex **3** exhibited the fastest CO-releasing rate herein whereas complex **1** showed the slowest. Overall, the photoinduced decomposition efficiency is poor for red light owing to essentially no absorption for long wavelength light in the visible region by the complexes. Although close examination of this region showed that complex **3** absorbs more than the other two in this region (Figure 3, inset), this may not be sufficient to explain this reversed trend from complexes **1** to **3** upon the illumination of the red light. One possible explanation is that this may be associated with the vibrational excited state related to the molecular orbital (HOMO) of complex **3**, since it was reported that vibrationally excited molecules are more reactive.[19] Whether the red light promoted CO release from complex **1** in DMSO could be attribute to this is not clear at this stage and needs further investigation which is currently undergoing in our laboratory.

Photoinduced CO release in D_2O and physiological saline–D_2O

Considering the potential for clinical application, we examined the kinetics of CO release from these complexes in water as well as in physiological saline. To eliminate the interference from H_2O in monitoring the IR spectral changes in the CO-releasing process, deuterated water was used, as we reported previously.[8d] Owing to the similar kinetic behaviour of complexes **1**–**3** upon photoinduction in DMSO, only complex **1** in D_2O and physiological saline (D_2O) under the illumination of blue light were examined. The IR spectral variations of the CO release from complex **1** under the illumination of blue light in D_2O and physiological saline are shown in Figure 9 and the Supporting Information, Figure S16, respectively. Compared to those observed in DMSO, the characteristic IR absorption bands of complex **1** showed red-shifts from 2043 and 1993 cm^{-1} to 2058 and 2012 cm^{-1}, respectively, in deuterated water.

In contrast to the behaviour in DMSO (Figure 5) under the illumination of blue light, the characteristic IR absorption bands steadily weakened, and two new peaks at 2125 and 2077 cm^{-1} emerged. Close inspection of the spectral variations revealed the conversion from the parent complex (**1**) into the intermediate

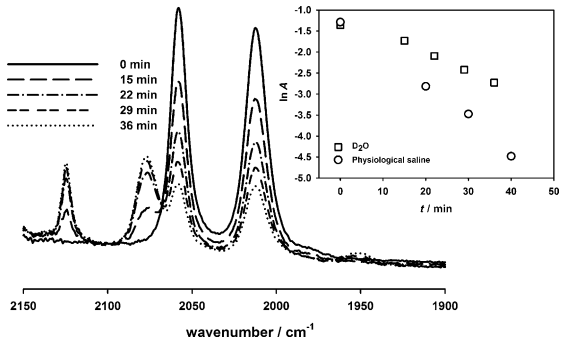

Figure 9. Variation of IR spectra during the decomposition of complex **1** (0.013 mol L^{-1}) under the blue-light illumination in D_2O and the decrease in the absorption at 2058 cm^{-1} with reaction time in D_2O and physiological saline, respectively (inset).

possessing new absorption bands. The spectral feature indicates that it must possess a core of {Fe^{II}(*cis*-CO)$_2$} (Figure 9). Furthermore, the same species was also observed in the physiological saline. However, both the conversion and the direct decomposition of complex **1** were facilitated (Table 2) in the

Table 2. Kinetic data of the photoinduced decomposition of complex **1** (0.013 mol L^{-1}) in D_2O and physiological saline (D_2O) upon blue-light illumination.

	D_2O	Physiological saline (D_2O)
$k_{obs} \times 10^3$	46 ± 6	66 ± 2

saline. Since the half-life time of the newly formed species was less than an hour, it was impossible to isolate this species for further identification. However, it was plausible to deduce its possible composition by overall consideration of the spectral variations in the three media (DMSO, D_2O, and physiological saline). The blue-shift by about 30 cm^{-1} indicates that the iron(II) centre of the species is of less electronic density. That no analogous species was observed in DMSO and the presence Cl^- speeded up its formation imply that both D_2O and Cl^- were involved in the formation of the species (Table 2). In combination with the mechanistic investigation of the CO release in DMSO, the most likely scenario is that the newly formed species might bear no Cp ring and the rest of the coordination around the metal centre was possibly satisfied by D_2O and/or Cl^-. Indeed, in the MS spectrum, fragments containing the

core $\{Fe(CO)_2\}$ were observed (Supporting Information, Figure S13) as discussed earlier. For example, the signal at 214.75 may be assigned to the fragment $[Fe(CO)_2Cl_2(CH_3OH)]^+$. The cleavage of the Cp ring is in agreement with the increase in wavenumber observed for the intermediate.

Synergetic CO release concerted by photoinduction and chemical reaction

As discussed above, the kinetic analysis revealed that the photoinduced reaction complies with a first-order reaction model. This is completely at odds with the kinetics expected of a photochemical reaction, since a photochemical reaction is zero-order. The results imply that in addition to the photoinduced reaction, there was a further driving forces to promote the CO release. As the media in which the reaction was performed were DMSO or D_2O, what occurred was probably that the solvents took part in the reaction to promote the CO release as discussed above. Both DMSO and water can coordinate to a transition-metal ion, including Fe^{II}. Therefore, it is not surprising that these solvents were involved in the CO-releasing reaction. To further confirm the involvement of the solvents in the CO release, the photoinduced reaction was performed in a non-polar solvent such as dichloromethane at three concentrations (Table 3). The derived k_{obs} was essentially constant (4.8 ± 0.4),

Table 3. The apparent rate constant and half-time ($t_{1/2}$, min) of the photoinduced decomposition of complex **1** in CH_2Cl_2 and CH_2Cl_2 + pyridine under different concentrations under blue-light illumination.

[**1**] [mol L^{-1}]	$K_{obs} \times 10^3$ ($t_{1/2}$ [min])	
	CH_2Cl_2	CH_2Cl_2 + Pyridine
0.013	4.5 ± 0.3 (27.5)	40 ± 6 (16.0)
0.025	4.8 ± 0.1 (56.3)	19 ± 1 (36.3)
0.038	5.2 ± 1 (81.8)	12.2 ± 0.8 (56.8)

which suggests that the reaction followed essentially the expected zero-order model. In our previous reports,[8d] we showed that a substitution reaction could solely cause diiron carbonyl complexes to decompose to release CO. To examine whether a similar reaction existed in this case, 20 equivalents of pyridine was added into the system. It turned out that the added pyridine worked to decompose the complex only with the help of illumination (Figure 10). The pyridine alone did not essentially decompose the complex. This suggests that pyridine worked on the excited species, **1***, rather than the ground state. The same is true in both D_2O and physiological saline (D_2O). In the absence of light, complex **1** exhibits a lack of decomposition in both media (Supporting Information, Figure S17 and S18). Therefore, based on what is described above, the overall scenario of the photoinduced CO release in coordinating media could be further developed into the mechanisms depicted in Scheme 2.

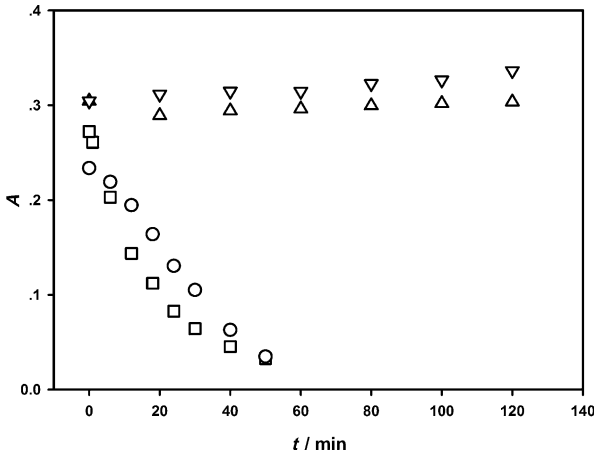

Figure 10. Plots of the absorbance at 2043 cm^{-1} of complex **1** (0.013 mol L^{-1}) against reaction time in CH_2Cl_2 under various reaction conditions: △ pyridine (20 equiv) with no illumination; ▽ no pyridine and no illumination; □ pyridine (20 equiv) under blue-light illumination; ○ illumination only.

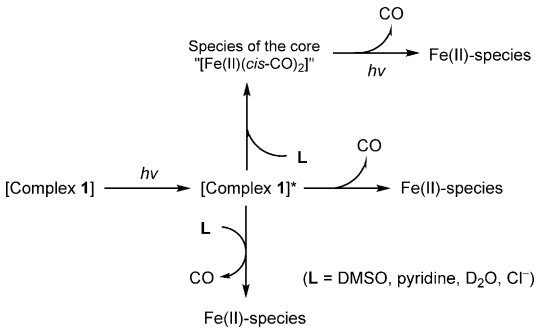

Scheme 2. Synergetic CO-releasing pathways in concert with photoinduction and chemical reactions.

Cytotoxicity of the CO-releasing system

To examine the biocompatibility of complexes **1**–**3** in the dark and under illumination, normal human liver cell line (QSG-7702) was employed to assess the cytotoxicity using MTT assay. IC_{50} values for complexes **1**–**3** were estimated at 384, 650, and 340 μmol L^{-1}, respectively (Supporting Information, Figure S19). Under the illumination of blue light, complexes **1**–**3** showed IC_{50} values as 375, 630, and 73 μmol L^{-1}, respectively (Supporting Information, Figure S20). The results show that all the complexes **1**–**3** are of low cytotoxicity. As for the phototoxicity, the three complexes behaved somewhat differently under illumination of the blue light. For both the chloro and bromo analogues, no significant change in cytotoxicity was observed, whereas for the iodo complex, its IC_{50} value is about 5-fold smaller. Whether this is relevant to its odd behaviour of CO release under the illumination of red light is not known.

Conclusion

Three iron(II) half-sandwich carbonyl complexes $[Fe(\eta^5\text{-Cp})(cis\text{-}CO)_2X]$ (X = Cl^-, Br^-, I^-) as PhotoCORMs have been investigated

in DMSO, D_2O, and physiological saline/D_2O. All the complexes release CO under illumination of visible light (blue, green, and red). The CO-releasing efficiency under photoinduction by either blue or green light decreased in the order of **1** (Cl^-), **2** (Br^-), and **3** (I^-). Their photoinduced CO release probably proceeds via two mechanisms, namely the direct decomposition induced by the illumination and the reaction of the excited species with solvent or other nucleophiles. In other words, the involvement of a nucleophile promotes the photoinduced decomposition probably in a concerted manner. On the other hand, the auxiliary ligands of the complexes exert a profound influence on their CO-releasing behaviour through altering the bonding nature of the metal–ligand bond and the energy levels of the frontier orbitals that are associated with the reduction potentials of the complexes. As a category of iron(II) complexes with the core {Fe^{II}(*cis*-CO)$_2$}, there is much space to manoeuvre in altering the auxiliary ligand(s) since there is a further fourth coordination number to be satisfied. Along with the low cytotoxicity of the examined complexes in normal human liver cell line (QSG-7702) with/without illumination, the prospect of this type of iron(II) carbonyl complexes is extremely promising as potential PhotoCORMs and worthy of further exploration.

It is of particular interest to mention the behaviour of the red light on inducing CO release from the three complexes. Although the CO release under illumination of red light was not as effective as the other two lights, it did induce CO release and, the order of releasing efficiency was reversed in the order of **3** (I^-), **2** (Br^-), and **1** (Cl^-). This could be attributed to the red light exciting the molecule to an overtone energy level of a certain bond of the complex which is, therefore, activated to react with the solvent (nucleophile) to release CO. This would offer us a novel approach to employ low-energy irradiation, including irradiation in the near-IR region, to initiate CO release by combining with the substitution reaction.

Experimental Section

Materials and instrumentation

Unless otherwise stated, all operations were carried out under an Ar atmosphere using standard Schlenk techniques. Reaction vessels were oven-dried at 150 °C and solvents were freshly distilled using the appropriate drying agent prior to use. $Fe(CO)_5$ and dicyclopentadiene were purchased from Aladdin and used as received to prepare [{CpFe(μ-CO)(CO)}$_2$] by following the previously reported procedure.[20] Complexes **1**–**3** were synthesised by following the procedures described previously with some modifications when necessary.[15] Measures for light shielding was taken during the synthesis and handling of the complexes owing to their light sensitivity. FTIR spectra in a solution were recorded on Agilent 640 using a CaF_2 cell with a spacer of 0.1 mm. UV/Vis spectra were measured on an Evolution 201 (Thermo Fisher Scientific). NMR spectra were measured on a Varian 400-MR spectrometer with tetramethylsilane as internal standard. Mass spectral data (ESI, positive mode) were collected on LCQ (Finnigan). Electrochemistry was performed in [tBu$_4$N]BF_4–CH_3CN by using a gas-tight and self-designed electrochemical cell. Potentials are quoted against the ferrocene couple. Detailed procedures for electrochemistry can be found elsewhere.[21] For illumination, LED light sources (red: $\lambda = 622$–770 nm; green: $\lambda = 492$–577 nm; and blue: $\lambda = 470$–475 nm; 60 LED clusters, 3 W, 220 V) were used. The set-up was placed in a cardboard box to shield off any unwanted light such as daylight.

Synthesis of complexes 1–3

[(η^5-C_5H_5)Fe(*cis*-CO)$_2$Cl] (**1**): Concentrated HCl (12 mol L^{-1}, 5 mL) was added to a solution of [{CpFe(μ-CO)(CO)}$_2$][20] (0.5 g, 1.4 mmol) in ethanol (30 mL). After being stirred overnight, the solvent was removed under reduced pressure to produce a residue that was purified with column chromatography (eluent: ethyl acetate/petroleum ether 1:4) to produce a red solid (yield: 234 mg, 1.1 mmol, 40 %). IR (CH_2Cl_2, $\tilde{\nu}_{CO}$/cm^{-1}): 2049, 2004; ^{1}H NMR ($CDCl_3$, ppm): 5.04 (5 H, Cp-*H*).

[(η^5-C_5H_5)Fe(*cis*-CO)$_2$Br] (**2**): Complex **2** was synthesised analogously to complex **1** by using HBr (6.8 mol L^{-1}, 5 mL) rather than HCl (yield: 334 mg, 1.3 mmol, 45 %). IR (CH_2Cl_2, $\tilde{\nu}_{CO}$/cm^{-1}): 2054, 2007; 1H NMR ($CDCl_3$, ppm): 5.03 (5 H, Cp-*H*).

[(η^5-C_5H_5)Fe(*cis*-CO)$_2$I] (**3**): A solution of I_2 (500 mg, 2.0 mmol) in CH_2Cl_2 (40 mL) was added dropwise to a flask charged with [{CpFe(μ-CO)(CO)}$_2$] (0.5 g, 1.4 mmol). The reaction was stirred continuously at room temperature for 2 h. The mixture was washed with $Na_2S_2O_3$ (0.13 mol L^{-1}, 2×70 mL) and H_2O_2 (5 %, 10 mL) water solution, respectively. The removal of the solvents under reduced pressure gave a crude product which was then purified with column chromatography (eluent: ethyl acetate/petroleum ether 1:4) to produce a dark-red solid (yield: 668 mg, 2.2 mmol, 80 %). IR (CH_2Cl_2, $\tilde{\nu}_{CO}$/cm^{-1}): 2041, 1997; ^{1}H NMR ($CDCl_3$, ppm): 5.03 (5 H, Cp-*H*).

Monitoring the CO release

A typical procedure for the monitoring is as follows: A solution of complex **1** (8.0 mg, 0.038 mmol) in DMSO (3.0 mL) was exposed to a LED light (blue: $\lambda = 470$–475 nm; green: $\lambda = 492$–577 nm and red: $\lambda = 622$–770 nm, 60 LED clusters, 3 W, 220 V). The set-up was placed in a cardboard box to shield off any unwanted lights. The light source was positioned right above the solution at a distance of 13 cm. The reaction was regularly monitored using IR spectroscopy. The same procedure was used to monitor the CO release in either D_2O or physiological saline in D_2O (NaCl, 0.15 mol L^{-1}). In both media, a small amount of DMSO (0.5 mL) was added to enhance the solubility of the complexes.

Cytotoxicity assessment using MTT assay

QSG-7702 cells (100 μL, 5×10^3 cells mL^{-1}) were seeded into 96-well plates and left to adhere for 24 h. The media was removed from the wells and replaced with fresh media containing the iron(II) complexes with different concentrations (100, 200, 300, 400, 500, 600, 700, 800, 900, and 1000 μmol L^{-1}), respectively. The cells were then incubated for another 24 h before the incubation media were replaced with the complete medium, and MTT (10 μL, 5 mg mL^{-1} in phosphate buffer solution, PBS) was added to each well of the plate. The cells were further incubated for 4 h before the media were replaced with DMSO (100 μL). Absorbance at 490 nm for each well of the plates was recorded with a microplate reader. In the MTT assay, DMSO (100 μL) in a well was used as blank and cells in the well without the addition of any complexes were taken as a control (100 % in cell viability). Relative cell viability is expressed as $(A_{obs}-A_b)/(A_c-A_b)$, where A_{obs}, A_b, and A_c are the absorbance observed for the cells treated with the complexes, blank, and the control, respectively. Inhibiting rate (%) was calculated as

100−[(A_{obs}−A_b)/(A_c−A_b)×100]. Each concentration was assayed in 5 wells of the same plate, which was repeated three times to examine the reproducibility of the assessment. IC_{50} values were estimated by using calibrating curve of inhibiting rate against the concentration. For the photocytotoxicity assay of complexes **1**–**3**, the procedure was similar to the above procedure, except that the 96-well plates were irradiated by blue LED light for 15 min before cultivation.

Acknowledgements

We thank the Natural Science Foundation of China (Grant Nos. 21102056, 21171073), the Government of Zhejiang Province (Qianjiang Professorship for X.L.), and the Graduate Innovation Fund of Jiangxi University of Science and Technology (Grant No. YC2013-X06, L.C.) for supporting this work. Professor Carl Redshaw at the University of Hull (UK) is also thanked for his language polishing of this manuscript.

Keywords: anions · carbon monoxide · carbonyl complexes · iron · photoinduction

[1] a) N. Schallner, L. E. Otterbein, *Front. Plant Physiol.* **2015**, *6*, 1 – 7 (article 17); b) B. Wegiel, D. W. Hanto, L. E. Otterbein, *Trends Mol. Med.* **2013**, *19*, 3 – 11; c) J. Louise Wilson, H. E. Jesse, R. K. Poole, K. S. Davidge, *Curr. Pharm. Biotechnol.* **2012**, *13*, 760 – 768; d) R. Motterlini, L. E. Otterbein, *Nat. Rev. Drug Discovery* **2010**, *9*, 728 – 743.

[2] B. S. Zuckerbraun, B. Y. Chin, B. Wegiel, T. R. Billiar, E. Czsimadia, J. Rao, L. Shimoda, E. Ifedigbo, S. Kanno, L. E. Otterbein, *J E.xp. Med.* **2006**, *203*, 2109 – 2119.

[3] a) R. Motterlini, *Circ. Res.* **1998**, *83*, 568; b) J. Kohmoto, A. Nakao, T. Kaizu, A. Tsung, A. Ikeda, K. Tomiyama, T. R. Bilhar, A. M. K. Choi, N. Murase, K. R. McCurry, *Surgery* **2006**, *140*, 179 – 185; c) G. Li Volti, L. F. Rodella, C. Di Giacomo, R. Rezzani, R. Bianchi, E. Borsani, D. Gazzolo, R. Motterlini, *Nephron Exp. Nephrol.* **2006**, *104*, e135 – e139.

[4] F. B. Mayr, A. Spiel, J. Leitner, C. Marsik, P. Germann, R. Ullrich, O. Wagner, B. Jilma, *Am. J. Respir. Crit. Care Med.* **2005**, *171*, 354 – 360.

[5] R. Motterlini, J. E. Clark, R. Foresti, P. Sarathchandra, B. E. Mann, C. J. Green, *Circ. Res.* **2002**, *90*, 17e – 24e.

[6] a) C. C. Romão, W. A. Blaettler, J. D. Seixas, G. J. L. Bernardes, *Chem. Soc. Rev.* **2012**, *41*, 3571 – 3583; b) T. R. Johnson, B. E. Mann, J. E. Clark, R. Foresti, C. J. Green, R. Motterlini, *Angew. Chem. Int. Ed.* **2003**, *42*, 3722 – 3729; *Angew. Chem.* **2003**, *115*, 3850 – 3858; c) U. Schatzschneider, *Br. J. Pharmacol.* **2015**, *172*, 1638 – 1650; d) S. H. Heinemann, T. Hoshi, M. Westerhausen, A. Schiller, *Chem. Commun.* **2014**, *50*, 3644 – 3660; e) B. E. Mann, *Top Organomet. Chem.* **2010**, *32*, 247 – 285.

[7] R. Motterlini, P. Sawle, S. Bains, J. Hammad, R. Alberto, R. Foresti, C. J. Green, *FASEB J.* **2005**, *19*, 284 – 286.

[8] a) T. R. Johnson, B. E. Mann, I. P. Teasdale, H. Adams, R. Foresti, C. J. Green, R. Motterlini, *Dalton Trans.* **2007**, 1500 – 1508; b) X. J. Jiang, L. Long, H. L. Wang, L. M. Chen, X. M. Liu, *Dalton Trans.* **2014**, *43*, 9968 – 9975; c) L. Chen, X. Jiang, X. Wang, L. Long, J. Zhang, X. Liu, *New J. Chem.* **2014**, *38*, 5957 – 5963; d) L. Long, X. Jiang, X. Wang, Z. Xiao, X. Liu, *Dalton Trans.* **2013**, *42*, 15663 – 15669.

[9] a) S. Romanski, B. Kraus, U. Schatzschneider, J.-M. Neudörfl, S. Amslinger, H.-G. Schmalz, *Angew. Chem. Int. Ed.* **2011**, *50*, 2392 – 2396; *Angew. Chem.* **2011**, *123*, 2440 – 2444; b) E. Stamellou, D. Storz, S. Botov, E. Ntasis, J. Wedel, S. Sollazzo, B. K. Kramer, W. van Son, M. Seelen, H. G. Schmalz, A. Schmidt, M. Hafner, B. A. Yard, *Redox Biol.* **2014**, *2*, 739 – 748.

[10] F. Zobi, O. Blacque, R. A. Jacobs, M. C. Schaub, A. Y. Bogdanova, *Dalton Trans.* **2012**, *41*, 370 – 378.

[11] a) J. S. Ward, J. M. Lynam, J. Moir, I. J. S. Fairlamb, *Chem. Eur. J.* **2014**, *20*, 15061 – 15068; b) M. A. Gonzales, P. K. Mascharak, *J. Inorg. Biochem.* **2014**, *133*, 127 – 135; c) I. Chakraborty, S. J. Carrington, P. K. Mascharak, *ChemMedChem* **2014**, *9*, 1266 – 1274; d) I. Chakraborty, S. J. Carrington, P. K. Mascharak, *Acc. Chem. Res.* **2014**, *47*, 2603 – 2611; e) R. D. Rimmer, A. E. Pierri, P. C. Ford, *Coord. Chem. Rev.* **2012**, *256*, 1509 – 1519.

[12] a) J. Zhao, Z. Wei, X. Zeng, X. Liu, *Dalton Trans.* **2012**, *41*, 11125 – 11133; b) Z. Y. Xiao, Z. H. Wei, L. Long, Y. L. Wang, D. J. Evans, X. M. Liu, *Dalton Trans.* **2011**, *40*, 4291 – 4299; c) Y. Tang, Z. H. Wei, W. Zhong, X. M. Liu, *Eur. J. Inorg. Chem.* **2011**, 1112 – 1120; d) Y. W. Wang, Z. M. Li, X. H. Zeng, X. F. Wang, C. X. Zhan, Y. Q. Liu, X. R. Zeng, Q. Y. Luo, X. M. Liu, *New J. Chem.* **2009**, *33*, 1780 – 1789; e) F. F. Xu, C. Tard, X. F. Wang, S. K. Ibrahim, D. L. Hughes, W. Zhong, X. R. Zeng, Q. Y. Luo, X. M. Liu, C. J. Pickett, *Chem. Commun.* **2008**, 606 – 608; f) C. Tard, X. M. Liu, S. K. Ibrahim, M. Bruschi, L. De Gioia, S. C. Davies, X. Yang, L. S. Wang, G. Sawers, C. J. Pickett, *Nature* **2005**, *433*, 610 – 613.

[13] X. F. Wang, Z. M. Li, X. R. Zeng, Q. Y. Luo, D. J. Evans, C. J. Pickett, X. M. Liu, *Chem. Commun.* **2008**, 3555 – 3557.

[14] S. Shima, R. K. Thauer, *Chem. Rec.* **2007**, *7*, 37 – 46.

[15] a) R. K. A. R. M. P. T. Murray, *J. Organomet. Chem.* **1987**, *323*, 53 – 65; b) A. R. Manning, G. McNally, D. Cunningham, P. McArdle, J. M. Simmie, *J. Organomet. Chem.* **1988**, *338*, 383 – 392; c) D. Serra, M. C. Correia, L. McElwee-White, *Organometallics* **2011**, *30*, 5568 – 5577.

[16] A. J. Bard, L. R. Faulkner, Electrochemical Methods: Fundamentals and Applications (2nd ed.), John Wiley & Sons, New York, **2000**, p. 4.

[17] N. J. R. van Eikema Hommes, T. Clark, *J. Mol. Model.* **2005**, *11*, 175 – 185.

[18] S. Imachi, M. Onaka, *Tetrahedron Lett.* **2004**, *45*, 4943 – 4946.

[19] F. F. Crim, *Proc. Natl. Acad. Sci. USA* **2008**, *105*, 12654 – 12661.

[20] Z. Teixeira, S. P. Vasconcellos, L. Koike, G. H. M. Dias, *Quim. Nova* **2007**, *30*, 494 – 496.

[21] X. Zeng, Z. Li, Z. Xiao, Y. Wang, X. Liu, *Electrochem. Commun.* **2010**, *12*, 342 – 345.

Received: April 7, 2015
Revised: May 19, 2015
Published online on July 27, 2015